J Therm Anal Calorim (2017) 130:1653–1661
DOI 10.1007/s10973-017-6580-1

# Kinetics studies of the degradation of sirolimus in solid state and in liquid medium

**M. S. T. Campos[1] · S. L. Fialho[2] · B. G. Pereira[2] · M. I. Yoshida[3] · M. A. Oliveira[1]**

Received: 9 December 2016 / Accepted: 14 July 2017 / Published online: 28 July 2017


**Abstract** The use of sirolimus and its analogs has been evaluated for the treatment of different cancer types. The stability studies of sirolimus enabled to determine the kinetics of its chemical reactions in solid state and in the liquid medium. During intrinsic stability tests in a liquid medium, sirolimus showed a lack of stability when exposed to heat, neutral and basic hydrolysis. Analysis by high-performance liquid chromatography detected: two degradation products after exposure to heat; one degradation product for both basic and neutral hydrolyses; and all degradation products exhibited UV spectra similar to the drug's spectrum. Kinetics studies in a liquid medium revealed low drug stability in methanolic solution; this instability may be exacerbated in the presence of water or high pH. The application of solid-state kinetic models showed that the drug degrades in accordance with the diffusion dimensional model, with greater stability and an expiration date equal to 6 years, demonstrating that sirolimus has satisfactory stability in the solid state. Through this understanding, it is possible to develop more stable pharmaceutical formulations using sirolimus.

**Keywords** Sirolimus · Thermal analysis · Chromatography · Degradation kinetics

## Introduction

Sirolimus (SRL) and its analogs have shown great potential as a new alternative for cancer treatment. In the early 1970s, the drug sirolimus was discovered as part of a screening program for new anti-microbial agents. The compound was first named rapamycin because it was isolated from a soil sample from the island Rapa Nui in Chile [1, 2]. SRL is a macrocyclic lactone (Fig. 1) produced as a secondary metabolite by the *Streptomyces hygroscopicus*. It is a crystalline solid with molecular weight 914.17 g $mol^{-1}$, and its color may vary from white to off-white. SRL was originally used as an antifungal agent against *Candida albicans* and subsequently its potent immunosuppressant and antiproliferative activities were determined [3–6].

SRL is practically insoluble in water, highly soluble in ethanol, chloroform, acetone and acetonitrile, and soluble in methanol and tetrahydrofuran. Its low solubility in water is a limitation factor for oral absorption [6–8].

SRL and its analogs have been evaluated for the treatment of the most common cancer types [5, 8–10], using both in vitro and in vivo studies. These studies include the inhibition of mTOR by sirolimus suppresses hypoxia-mediated angiogenesis and endothelial cell proliferation in vitro [11]. In in vivo mouse models, sirolimus demonstrates powerful inhibitory effects on tumor growth and angiogenesis [12]. SRL strongly inhibits cell proliferation

**Electronic supplementary material** The online version of this article (doi:10.1007/s10973-017-6580-1) contains supplementary material, which is available to authorized users.

✉ M. A. Oliveira
oliveirama.ufes@gmail.com

[1] Centro Universitário Norte do Espírito Santo, UFES, Rodovia BR 101 Norte, Km 60, Bairro Litorâneo, 29932-540 São Mateus, ES, Brazil

[2] Fundação Ezequiel Dias, FUNED, R. Conde Pereira Carneiro, Bairro Gameleira, 30510-010 Belo Horizonte, MG, Brazil

[3] Departamento de Química, Universidade Federal de Minas Gerais, Av. Presidente Antônio Carlos, 6627, 31270-901 Belo Horizonte, MG, Brazil

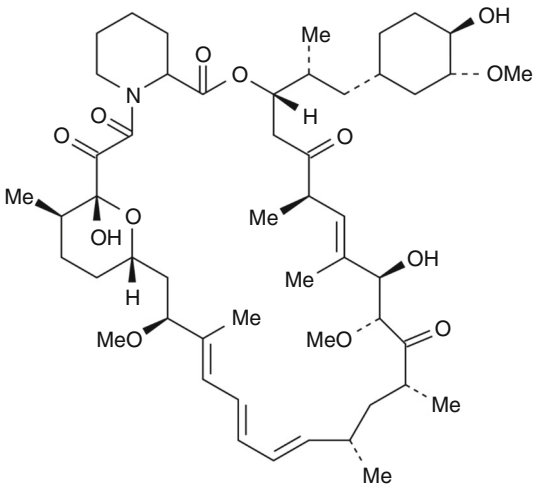


**Fig. 1** Structural formula of sirolimus

in cell lines derived from rhabdomyosarcoma [13, 14], neuroblastoma, glioblastoma [15], osteosarcoma [16], small cell lung cancer [17], pancreatic cancer [18], breast cancer, prostate cancer [19, 20], murine melanoma and B cell lymphoma [21, 22]. However, the clinical development of a formulation, which combines effectiveness with low toxicity, has been a challenge because the drug has poor water solubility and chemical stability [6]. The kinetics studies of drug degradation in solid-state and in a liquid medium are able to support the development these pharmaceutical formulations with high stability and compatible with excipients.

## Intrinsic stability and determination of degradation kinetics in liquid medium

During the development of pharmaceutical formulations, it is important to determine the drug intrinsic stability in anticipation of possible chemical reactions and degradation products [23, 24]. The drug stability should be evaluated under distinct temperature, humidity, oxidation, light exposure, hydrolysis and metallic ion conditions [23–25]. The photostability test can be evaluated under the conditions recommended by ICH Q1B [26] by subjecting the substance to ultraviolet irradiation. After submission of stress conditions, the samples are analyzed using analytical techniques with high sensibility such as high-performance liquid chromatography (HPLC). Degradation products and the substance's degradation extension can be determined using a reference standard, and some degradation pathways can be complex. Furthermore, not of all decomposition products formed under conditions of intrinsic stability can be observed in the drug when subjected to the official conditions of the stability studies [27, 28].

In addition to known aspects of the drug's intrinsic stability, the determination of the expiration date is one of the most important factors that should be evaluated during the course of pharmaceutical development. These studies are practiced routinely for the pharmaceutical industry, however, requires longs period of samples storage, under controlled conditions of temperature and humidity [29].

The degradation kinetic is also used to determine the drug stability, the extension of degradation, the $t_{90}$ (time to degrade 10% of the drug), the speed of reaction, and the degradation facility (which is related to the energy activation reaction). When compared with the drug's stress conditions analysis, these degradation kinetics studies become interesting, as they make possible the establishment of a proportionality logic for chemical reactions. The calculation for degradation kinetics in a liquid medium can be obtained applied to zero, first, and second order reactions in concordance with the linear regression coefficient ($r$) obtained by degradation curve. In concordance with the better adjusted model (zero, first or second order reactions), it is possible to calculate the reaction rate constant ($k$) for each temperature, using the inclination rate results and to proceed on the other kinetics calculations based on Arrhenius equation [30–37].

## Stability and degradation kinetics studies in solid-state

Although the conventional studies cannot be replaced, thermoanalytical techniques such a differential scanning calorimetry (DSC) are extremely relevant to the stability studies, since they make possible to choose quickly, through the compatibility studies and much more stable formulations. Thermogravimetry (TG) is another thermoanalytical technique used for evaluating stabilities of the drug and medicines and also for performing isothermal and non-isothermal kinetics studies [36–40].

The kinetics of degradation in solid state can be obtained by two methods: (1) isothermal or (2) non-isothermal/dynamic. Each one of these methods has specific mathematical models for adjustment that consider the degradation process and the order of the reaction. The use of Arrhenius equation is also advisable for calculating $t_{90}$, activation energy and the pre-exponential factor. The kinetic equations that delineate thermal decomposition are classified into different types of processes, and these processes are controlled by nucleation, diffusion mechanisms and reactions in the boundary phase, covering geometrical and physicochemical aspects, depending on the rate-determining step of the reaction [41].

The knowledge of the drug stability and its degradation products are a fundamental role during the development of pharmaceutical formulations. Considering this, the

objective of this project was to evaluate and understand the chemical stability of SRL for developing a new pharmaceutical formulation for cancer treatment.

## Experimental

High-performance liquid chromatography (Waters® alliance e2695) with an auto-injector, a diode-array detector UV/DAD, and a column oven was used in the analysis. For optimizing the methodology analysis [42, 43], were tested four types of reverse-phase chromatographic columns C8 and C18, in distinct temperatures of 30, 40 and 50 °C; and variations in wavelength and injection volume were also performed. The chromatographic conditions used in the analysis were: C18 column (250 × 4.6 mm, 5 µm, Varian); mobile phase containing methanol–water (80:20); flow at 1.5 mL $min^{-1}$; injection volume of 20 µL; UV detection at $\lambda = 278$ nm; and oven temperature at 50 °C.

### Drug degradation study in liquid medium (solution) by HPLC

The stress conditions (intrinsic stability) of SRL were systematically investigated after 4 h of exposure under distinct conditions in accordance with the RDC 58/13 [25] and ICH [23, 26]: (1) dry heat at 60 °C, (2) reflux over steam bath in water, (3) in NaOH 1 M, (4) in HCl 1 M, (5) in aqueous solution of $H_2O_2$ 3%, (6) UV light (254 nm) and (7) metallic ions in solution of $Fe^{2+}$ 0.05 M. For basic and acid drug degradation tests, the initial solutions were diluted to NaOH 0.0005 M and HCl 0.005 M, which allowed the detection of degradation products and detection of the drug in the samples. A standard stock solution of drug was prepared at a concentration of 0.1 mg $mL^{-1}$ and solubilized in methanol.

### Evaluation of degradation kinetics in liquid medium (solution)

For evaluation of the drug degradation kinetics in solution, additional tests were required applying distinct temperature and time for each interested stress condition, using quadruplicate samples. Additional tests are shown in Table 1.

Kinetics studies were conducted applying extrapolated calculations according to Arrhenius equation, for expiration date prediction at 25 °C. The samples submitted to stress were analyzed by HPLC and were determined, and the possible chemical reactions of the drug under stress were studied. After obtaining the analytical results, the order of the degradation reactions was established according to the models of zero, first, and second orders. These orders were determined by applying the linear correlation coefficient ($r$) and by calculating the reaction rate constant ($k$), using the aid of a straight slope for each temperature. With this calculated value of $k$, the activation energy ($E_a$) at 25 °C and the $k_{25°C}$ could be calculated, thereafter the time required for degrading 10% of the drug ($t_{90}$ drug) at 25 °C was estimated applying the graphical method of the Arrhenius equation. The slope of the line is defined by $E_a \times R^{-1}$, where the activation energy ($E_a$) was calculated by multiplying the slope by the universal gas constant ($R$) (8.314 J $mol^{-1}$ $K^{-1}$). The $E_a$ also expressed the drug stability, being directly proportional to stability.

The equations used to describe the kinetics of degradation in solution and the time required for degrading 10% of the drug ($t_{90}$ drug) at 25 °C are described in the following:

**Table 1** Additional degradation tests for evaluation the drug intrinsic stability

| Stress conditions | Aliquot collected | Temperature | | | |
|---|---|---|---|---|---|
| | | 50 °C $min^{-1}$ | 60 °C $min^{-1}$ | 70 °C $min^{-1}$ | 80 °C $min^{-1}$ |
| Heat | 1 | 60 | 60 | 45 | 30 |
| | 2 | 120 | 120 | 90 | 60 |
| | 3 | 180 | 180 | 135 | 90 |
| | 4 | 240 | 240 | 180 | 120 |
| Neutral hydrolysis | 1 | 60 | 60 | 60 | 60 |
| | 2 | 120 | 120 | 120 | 120 |
| | 3 | 180 | 180 | 180 | 180 |
| | 4 | 240 | 240 | 240 | 240 |
| Basic hydrolysis | 1 | 60 | 45 | 30 | 15 |
| | 2 | 120 | 90 | 60 | 30 |
| | 3 | 180 | 135 | 90 | 45 |
| | 4 | 240 | 180 | 120 | 60 |

Zero order:

$$C = -kT + \text{Co}$$
$$t_{90} = (0.1 \times \text{Co})/k$$

First order:

$$\ln C = -kT + \ln\ \text{Co}$$
$$t_{90} = 0.105/k$$

Second order:

$$1/C = kT + 1/\text{Co}$$
$$t_{90} = 1/(9 \times k \times \text{Co})$$

where $C$, concentration/%; $k$, rate constant ($s^{-1}$); Co, initial concentration; $t$, time/s.

Arrhenius equation:

$$\ln\ k = \ln\ A - \frac{-\text{Ea}}{R} \times \frac{1}{T}$$

where $k$ rate constant; $E_a$ activation energy; $A$ pre-exponential factor; $T$ temperature in Kelvin; $R$ gas constant (8.314 J $mol^{-1}$ $K^{-1}$).

**Table 2** Rate laws for reactions in solids

| Function symbol | Mechanism | Integral form $g(a)$ |
|---|---|---|
| Acceleratory $a \times t$ curves | | |
| Pn | Power law | $a^{1/n}$ |
| E1 | Exponential law | $\ln a$ |
| Sigmoidal $a \times t$ curves | | |
| A2 | Avrami–Erofeev two-dimensional growth of nuclei | $[-\ln (1 - a)]^{1/2}$ |
| A3 | Avrami–Erofeev three-dimensional growth of nuclei | $[-\ln (1 - a)]^{1/3}$ |
| A4 | Avrami–Erofeev | $[-\ln (1 - a)]^{1/4}$ |
| B1 | Prout–Tompkins | $\ln [a/(1 - a)]$ |
| Deceleratory $a \times t$ curves | | |
| Based on geometrical models | | |
| R2 | Contracting area | $1 - (1 - a)^{1/2}$ |
| R3 | Contracting volume | $1 - (1 - a)^{1/3}$ |
| Based on diffusion | | |
| D1 | One-dimensional diffusion | $a^2$ |
| D2 | Two-dimensional diffusion (Valensi equation) | $((1 - a) \ln(1 - a)) + a$ |
| D3 | Three-dimensional diffusion (Jander equation) | $[1 - (1 - a)^{1/3}]^2$ |
| D4 | Ginstling–Brounshtein | $[1 - (2a/3)] - (1 - a)^{2/3}$ |
| Based on reaction order | | |
| F0 | Zero order | $a$ |
| F1 | First order | $-\ln (1 - a)$ |
| F2 | Second order | $1/(1 - a)$ |
| F3 | Third order | $[1/(1 - a)]^2$ |

### Stability and degradation kinetics studies in solid-state

The kinetics of the solid state has specific mathematical models for adjustment considering the degradation process and the order of reaction, as described in Table 2. In this work, was used the isothermal method, which is widely used to monitor the kinetics of decomposition reactions in the solid state. TG curves were performed using thermobalance DTG 60 (Shimadzu, Japan). Three milligrams was placed in an aluminum crucible under a nitrogen flow rate of 50 mL $min^{-1}$. TG isothermal curves by SRL were obtained at previously established temperatures ($T$) taking into account the initial part of the SRL degradation 180, 182, 184, 186 and 188 °C, and graphs of time ($t$) versus fraction decomposed ($\alpha$) were prepared to evaluate the kinetics. Determined the best kinetic model describing the reaction study, further analysis at different temperatures allows calculating the activation energy by Arrhenius equation in linear form and predicts the shelf life at 25 °C [44].

## Results and discussion

### Drug degradation study in liquid medium (solution) by HPLC

Chromatographic conditions were optimized for analyzing the SRL and its degradation products. Was performed a partial validation of the methodology. Figure 2 shows two typical peaks that are corresponding to the tautomers pyran ($t_R$ = 6.0 min) and oxepan ($t_R$ = 7.5 min) [29, 32]. The methodology presented appropriate specificity, linearity, accuracy and precision results. SRL's system suitability calculated for pyran tautomer was: a capacity factor ($k'$) of 4.65; a theoretical plates/column ($N$) of 4520, a peak symmetry (As) of 1.02 and a resolution (Rs) between the tautomers equal to 5.6. The results were compared with established limits for each parameter [45].

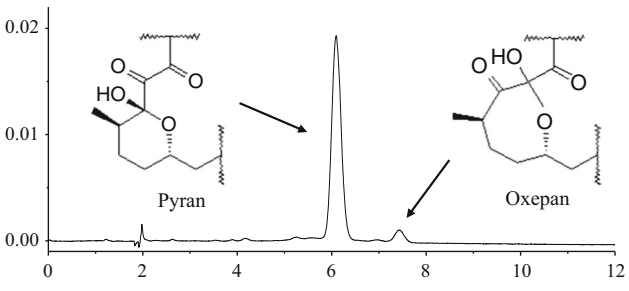


**Fig. 2** Tautomers pyran and oxepan

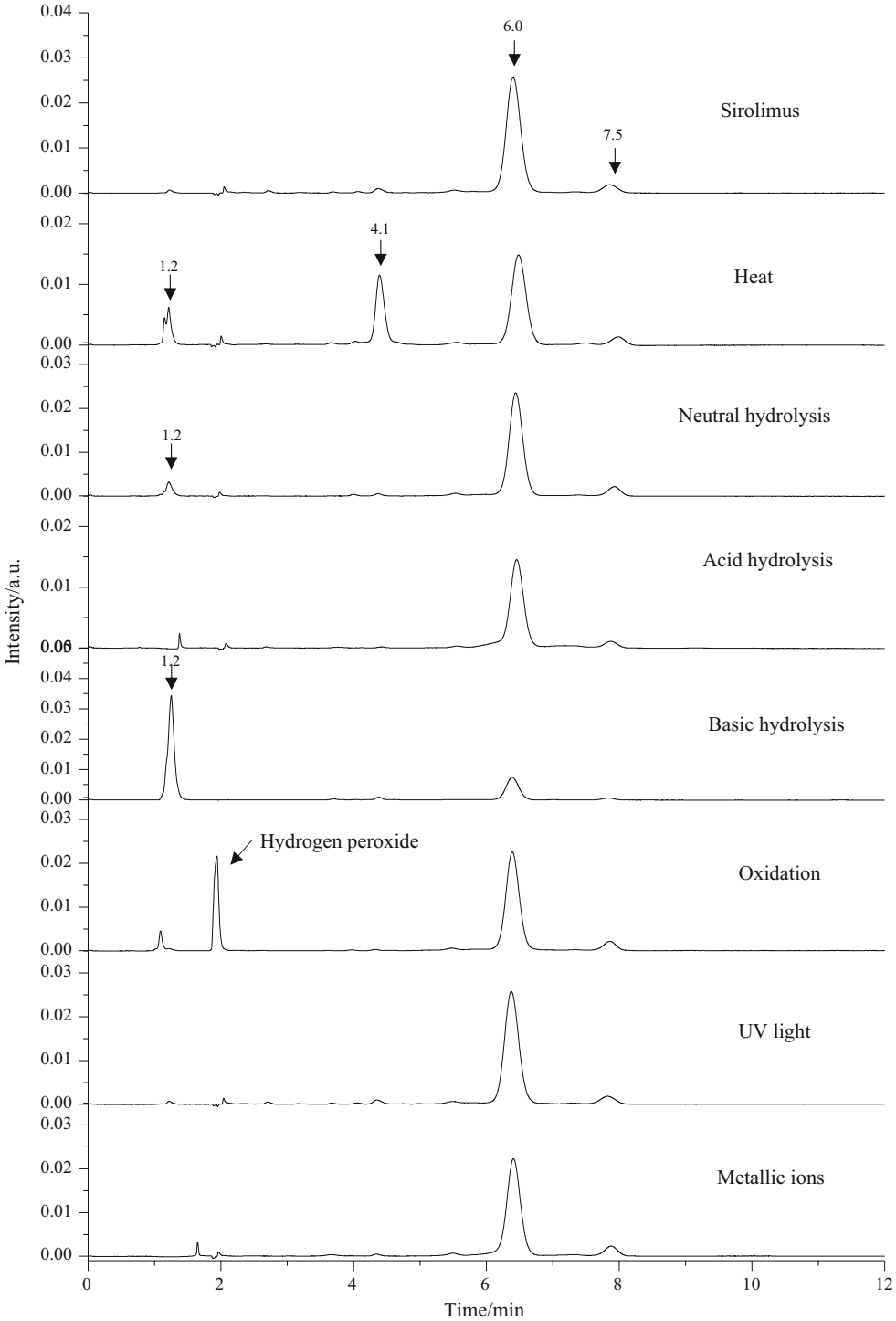


**Fig. 3** Sirolimus chromatograms before and after stress conditions: exposure to temperature (heat); neutral hydrolysis; acid hydrolysis; basic hydrolysis; oxidation; exposure to UV light; exposure to metallic ions

Figure 3 shows SRL chromatograms before and after stress conditions for intrinsic stability test. The degradation product (DP) with time retention ($t_R$) of 1.2 min, as seen in Figure 1S, is presented in the chromatograms for samples exposed to heat, basic and neutral hydrolysis. The results reveal a UV spectrum with great similarity to the SRL with the same $\lambda_{max}$, indicating that the structure of the chromophore remains the same in the degradation products. The degradation of SRL under heat condition produced another DP with $t_R$ of 4.1 min, and its spectrum also has great similarity with the SRL's spectrum (Figure 1S). Furthermore in the sample subjected to oxidation could be observed a peak with $t_R$ of 2.0 min that represents the peak of hydrogen peroxide.

**Table 3** Results of the mathematical models adjustment of zero, first, and second order, with values of $r$ (correlation coefficient) and $k$ (reaction rate) for forced degradation of SRL in heat

| Temperature/°C | Parameters | Order | | |
|---|---|---|---|---|
| | | Zero | First | Second |
| SRL forced degradation in heat | | | | |
| 50 | $r$ | 0.97861 | 0.98376 | 0.98785 |
| | $k$ | 4.81000 | 0.05383 | 0.00060 |
| 60 | $r$ | 0.99264 | 0.99592 | 0.99173 |
| | $k$ | 9.60300 | 0.12290 | 0.00160 |
| 70 | $r$ | 0.95261 | 0.98146 | 0.89907 |
| | $k$ | 33.46133 | 1.43017 | 0.17516 |
| 80 | $r$ | 1.00000 | 1.00000 | 1.00000 |
| | $k$ | 185.42000 | 5.32138 | 0.25435 |

**Table 4** Results of the mathematical models adjustment of zero, first, and second order, with values of $r$ (correlation coefficient) and $k$ (reaction rate) for neutral hydrolysis of SRL

| Temperature/°C | Parameters | Order | | |
|---|---|---|---|---|
| | | Zero | First | Second |
| Neutral hydrolysis of SRL | | | | |
| 50 | $r$ | 0.99763 | 0.99889 | 0.99966 |
| | $k$ | 3.55900 | 0.01669 | 0.00042 |
| 60 | $r$ | 0.99384 | 0.99519 | 0.99547 |
| | $k$ | 5.83200 | 0.02867 | 0.00075 |
| 70 | $r$ | 0.99002 | 0.99596 | 0.99916 |
| | $k$ | 7.26800 | 0.03756 | 0.00104 |
| 80 | $r$ | 0.99650 | 0.96909 | 0.93026 |
| | $k$ | 37.38500 | 0.29904 | 0.01482 |

Chromatograms for stress under heating (Figures 2S and 3S) showed that the increase in temperature and exposure time (additional tests) resulted in drug degradation, with the formation of two degradation products, DP1 ($t_R = 1.2$ min) and DP2 ($t_R = 4.3$ min). For neutral and basic hydrolyses (Figures 4S, 5S, 6S, and 7S), a single DP was observed ($t_R = 1.2$ min). Degradation test in acid medium showed also a DP with $t_R$ of 1.2 min, however, in a lower amount than other hydrolyses, which suggest that the reaction of DP formation occurred preferably at neutral and basic pH. Therefore, calculation of kinetic degradation in acid hydrolysis was not important for this work.

Considering the results in Table 1, was possible to obtain the degradation kinetics of the drug. Values of the mathematical model's adjustments of zero, first and second order for SRL under heat exposure, neutral and basic hydrolyses in the temperatures of 50, 60, 70 and 80 °C, are described in Tables 3–5, respectively.

**Table 5** Results of the mathematical models adjustment of zero, first, and second order, with values of $r$ (correlation coefficient) and $k$ (reaction rate) for basic hydrolysis of SRL

| Temperature/°C | Parameters | Order | | |
|---|---|---|---|---|
| | | Zero | First | Second |
| Basic hydrolysis of SRL | | | | |
| 50 | $r$ | 0.96982 | 0.97465 | 0.97880 |
| | $k$ | 4.90400 | 0.02379 | 0.00061 |
| 60 | $r$ | 0.97403 | 0.97432 | 0.96202 |
| | $k$ | 13.86667 | 0.08078 | 0.00257 |
| 70 | $r$ | 0.99347 | 0.99961 | 0.98765 |
| | $k$ | 30.09000 | 0.20129 | 0.00758 |
| 80 | $r$ | 0.96746 | 0.93220 | 0.90714 |
| | $k$ | 102.42400 | 1.35481 | 0.16512 |

During heat exposure, the first order represented the kinetics of best fit, which presented a linear correlation coefficient ($r$) close to 1.0000. These values are shown in Table 3. It was possible to calculate the $k_{25°C}$ by extrapolation that was 0.00033 mol $L^{-1}$ $s^{-1}$; the $t_{90}$ at 25 °C in a methanolic medium was 319.6 h or 13 days.

Figure 4 shows the graph of the Arrhenius equation, ln $k$ versus $1/T$. The graphical method of Arrhenius equation is the most widely used for the calculation of the kinetic parameters. The $E_a$ calculated for SRL under heat exposure condition was 153.53 kJ $mol^{-1}$.

During neutral hydrolysis, the second order represented the kinetics of best fit. These values are shown in Table 4. The $k_{25°C}$ calculated by extrapolation was $1.0 \times 10^{-5}$ mol $L^{-1}$ $s^{-1}$; the $t_{90}$ at 25 °C in a neutral medium was 101.24 h or 4.22 days, and the $E_a$ was 103.54 kJ $mol^{-1}$.

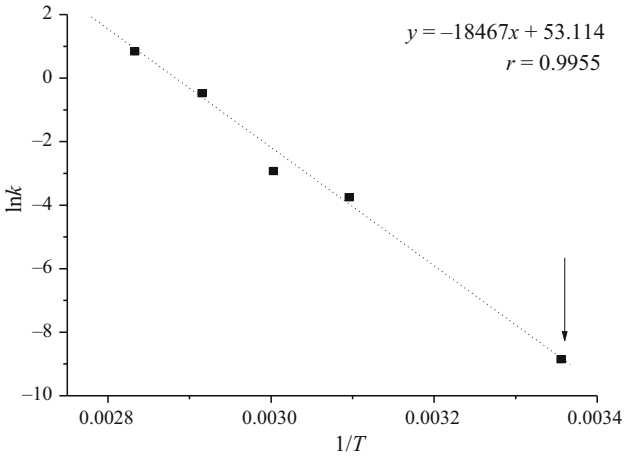


**Fig. 4** Graph of the Arrhenius equation—forced degradation of SRL in heat

**Table 6** Degradation kinetic calculation of SRL in solid state, with values of $r$ and $k$

| Temperature/°C | Parameters | Mathematical models for adjustment | | | | | | | | |
|---|---|---|---|---|---|---|---|---|---|---|
| | | A2 | A3 | A4 | B1 | R2 | R3 | D1 | D2 | D3 |
| 180 | $r$ | 0.7772 | 0.7296 | 0.7006 | 0.5983 | 0.7656 | 0.718 | 0.9392 | 0.9418 | 0.9443 |
| | $k$ | 0.0001 | 0.0001 | 0.0000 | 0.0004 | 0.0000 | 0.0000 | 0.0000 | 0.0000 | 0.0000 |
| 182 | $r$ | 0.8158 | 0.7700 | 0.7418 | 0.6389 | 0.807 | 0.7611 | 0.9649 | 0.9666 | 0.9682 |
| | $k$ | 0.0001 | 0.0001 | 0.0001 | 0.0011 | 0.0001 | 0.0001 | 0.0000 | 0.0000 | 0.0000 |
| 184 | $r$ | 0.7987 | 0.7517 | 0.7229 | 0.6189 | 0.7897 | 0.7426 | 0.9553 | 0.9572 | 0.959 |
| | $k$ | 0.0001 | 0.0001 | 0.0001 | 0.001 | 0.0001 | 0.0001 | 0.0000 | 0.0000 | 0.0000 |
| 186 | $r$ | 0.7816 | 0.7327 | 0.703 | 0.5981 | 0.771 | 0.7222 | 0.9495 | 0.9518 | 0.954 |
| | $k$ | 0.0001 | 0.0001 | 0.0001 | 0.0009 | 0.0001 | 0.0001 | 0.0000 | 0.0000 | 0.0000 |
| 188 | $r$ | 0.7754 | 0.7246 | 0.6939 | 0.5852 | 0.7647 | 0.7139 | 0.9489 | 0.9512 | 0.9534 |
| | $k$ | 0.0001 | 0.0001 | 0.0001 | 0.0008 | 0.0001 | 0.0001 | 0.0000 | 0.0000 | 0.0000 |
| Temperature/°C | Parameters | Continuation—mathematical models for adjustment | | | | | | | | |
| | | D4 | F0 | F1 | F2 | F3 | E1 | P2 | P3 | P4 |
| 180 | $r$ | 0.9427 | 0.8566 | 0.8672 | 0.8773 | 0.8869 | 0.5788 | 0.7656 | 0.718 | 0.6892 |
| | $k$ | 0.0000 | 0.0000 | 0.0000 | 0.0000 | 0.0001 | 0.0004 | 0.0000 | 0.0000 | 0.0000 |
| 182 | $r$ | 0.9671 | 0.8923 | 0.9001 | 0.9076 | 0.9148 | 0.6236 | 0.807 | 0.7611 | 0.733 |
| | $k$ | 0.0000 | 0.0001 | 0.0001 | 0.0001 | 0.0002 | 0.001 | 0.0001 | 0.0001 | 0.0001 |
| 184 | $r$ | 0.9578 | 0.878 | 0.8861 | 0.8939 | 0.9014 | 0.6033 | 0.7897 | 0.7426 | 0.7139 |
| | $k$ | 0.0000 | 0.0001 | 0.0001 | 0.0001 | 0.0001 | 0.0009 | 0.0001 | 0.0001 | 0.0001 |
| 186 | $r$ | 0.9525 | 0.8649 | 0.8747 | 0.884 | 0.8929 | 0.5807 | 0.771 | 0.7222 | 0.6927 |
| | $k$ | 0.0000 | 0.0001 | 0.0001 | 0.0001 | 0.0001 | 0.0008 | 0.0001 | 0.0001 | 0.0001 |
| 188 | $r$ | 0.9519 | 0.8619 | 0.8716 | 0.881 | 0.8899 | 0.5673 | 0.7647 | 0.7139 | 0.6833 |
| | $k$ | 0.0000 | 0.0000 | 0.0001 | 0.0001 | 0.0001 | 0.0007 | 0.0001 | 0.0001 | 0.0001 |

The kinetics of basic hydrolysis was zero order. These values are shown in Table 5. The $k_{25°C}$ calculated by extrapolation was 0.25357 mol $L^{-1}$ $s^{-1}$; the $t_{90}$ at 25 °C in a basic medium was 39.436 h or 1.64 days, and the $E_a$ was 93.64 kJ $mol^{-1}$.

## Solid-state degradation kinetics

The isothermal degradation kinetics was evaluated, using mathematical models adjusted for the thermal decomposition of solids, according to formulas described in Table 3. The results of the calculated parameters [linear correlation coefficient ($r$) and reaction rate ($k$)] are shown in Table 6.

The results showed that SRL degrades according to a diffusional model ($D$). The best regression coefficient was achieved with *diffusional dimensional* model D3, at all temperatures tested. This type of degradation occurs in cases where nucleation is instantaneous and the further reaction occurs by interpenetration of reagent particles, which is probably the determining step of the process speed [46]. Figure 5 shows the graph of the degree conversion ($\alpha$) for the time given in seconds. It can be seen that the higher the temperature used in the experiment, the faster the SRL begins to degrade and can subsequently watch the deceleration of this degradation with increasing time, which agrees with the model of diffusional setting (D3) which is a decelerating kinetic model.

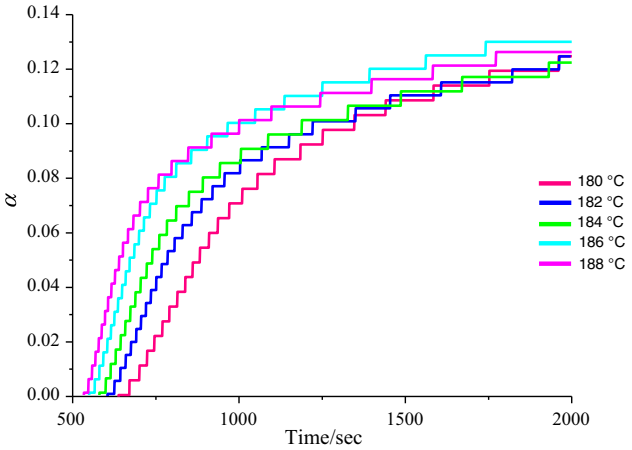


**Fig. 5** Graph of fraction decomposed for the time

To perform the activation energy calculation, was used the natural logarithm of time as a function of reciprocal

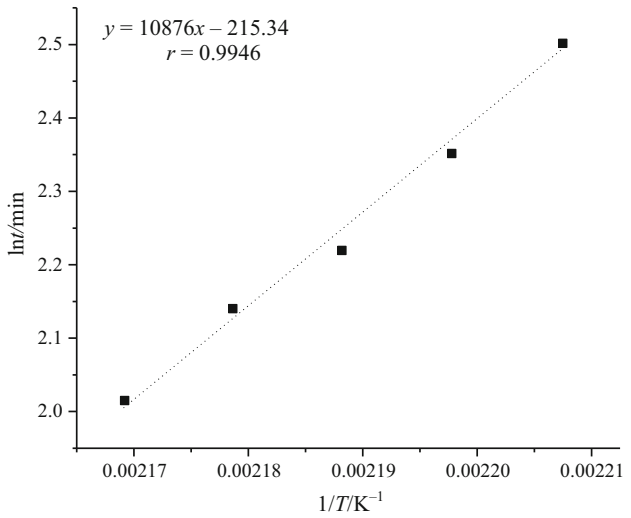


**Fig. 6** Arrhenius plot constructed from the results obtained from the isotherms at 10% SRL mass loss

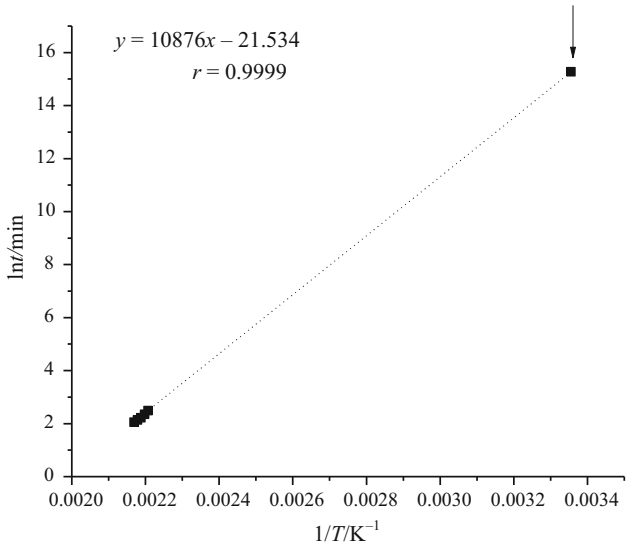


**Fig. 7** Arrhenius plot extrapolated to 10% SRL mass loss

temperature [ln $t$ (min) vs. $1/T$ ($K^{-1}$)]; for a construction of the Arrhenius graph was used a fixed drug mass loss of 10%. This type of calculation was performed because the diffusion adjustment model does not have described a classical kinetic reaction order, requiring, therefore, the use of an alternative method [47–49]. Figure 6 shows the graph obtained with the angulation value used in the calculation; this value achieved a correlation of $r = 0.9946$. The value of $E_a$ calculated was 90.42 kJ $mol^{-1}$.

The data obtained from the Arrhenius plot were extrapolated using a straight line at a temperature of 25 °C (Fig. 7), and the $t_{90}$ obtained by ln $t$ at 25 °C for 10% loss of SRL was 6 years.

## Conclusions

SRL demonstrated instability in solution and can be considered very unstable after methanol solubilization. For the intrinsic stability studies and the kinetic studies in solution, the sample of SRL exposed to heat showed partial degradation with first-order reaction kinetic and a formation of two degradation products. For hydrolysis conditions in neutral and basic medium, the drug also exhibited partial degradation, with a formation of one degradation product and second- and zero-order kinetics, respectively. These results demonstrate that the instability of the drug in solution may be exacerbated in the presence of heat, water and/or high pH.

In solid-state kinetics studies, SRL presented degradation predicted by diffusional dimensional model D3 with a deceleration kinetic, and the $E_a$ calculated was 90.42 kJ $mol^{-1}$ and with a $t_{90}$ of 6 years, which is considered a good result in terms of drug stability.

The understanding of the physical and chemical characteristics of the SRL, as the drug stability and degradation products, gives the needed support for the selection of the most fitting excipients for the development of a stable pharmaceutical formulation, which will assure a reduced risk to the patient with a greater effectiveness of the cancer treatment.

**Acknowledgements** The authors wish to thank Ezequiel Dias Foundation (FUNED) for providing the samples. National Council for the Improvement of Higher Education (CAPES), National Council for Scientific and Technological Development (CNPq) and the Research Support Foundation of the Espirito Santo (FAPES) for financial support.

## References

1. Sehgal SN. Rapamune (Sirolimus, rapamycin): an overview and mechanism of action. Ther Drug Monit. 1995;17:660–5.
2. Hartford CM, Ratain MJ. Rapamycin: something old, something new, sometimes borrowed and now renewed. Clin Pharmacol Ther. 2007;82:4.
3. Goodman LS, Gilman A. As bases farmacológicas da terapêutica. 11th ed. Rio de Janeiro: McGraw-Hill; 2006.
4. Sehgal SN, et al. Rapamycin (AY-22,989), a new antifungal antibiotic. II. Fermentation, isolation and characterization. J Antibiot. 1975;28:727–32.
5. Pópulo HIM. Dissertation. Relevance of mTOR pathway in the initiation/progression of human tumours. Universidade do Porto, Porto (2001).
6. Zhang Y, et al. Targeting the mTOR kinase domain: the second generation of mTOR inhibitrs. Drug Discov Today. 2011;16(7–8):325–31.
7. Solymosi T, et al. Research paper sirolimus formulation with improved pharmacokinetic properties produced by a continuous flow method. Eur J Pharm Biopharm. 2015;94:135–40.

8. Facompre ND. Remarkable inhibition of mTOR signaling by the combination of rapamycin and 1,4-phenylenebis(methylene)selenocyanate in human prostate cancer cells. Int J Cancer. 2012;131:2134–42.
9. Liu M, et al. Antitumor activity of rapamycin in a transgenic mouse model of ErbB2-dependent human breast cancer. Cancer Res. 2005;65:5325–36.
10. Stippel DL, et al. Successful use of sirolimus in a patient with bulky ovarian metastasis of hepatocellular carcinoma after liver transplantation. Transplant Proc. 2005;37:2185–7.
11. Humar R, et al. Hypoxia enhances vascular cell proliferation and angiogenesis in vitro via rapamycin (mTOR)-dependent signaling. FASEB J. 2002;16:771–80.
12. Guba M, et al. Rapamycin inhibits primary and metastatic tumor growth by antiangiogenesis: involvement of vascular endothelial growth factor. Nat Med. 2002;8:128–35.
13. Dilling MB, et al. Rapamycin selectively inhibits the growth of childhood rhabdomyosarcoma cells through inhibition of signaling via the type I insulin-like growth factor receptor. Cancer Res. 1994;54:903–7.
14. Hosoi H, et al. Rapamycin causes poorly reversible inhibition of mTOR and induces p53-independent apoptosis in human rhabdomyosarcoma cells. Cancer Res. 1999;59:886–94.
15. Geoerger B, et al. Antitumor activity of the rapamycin analog CCI-779 in human primitive neuroectodermal tumor/medulloblastoma models as single agent and in combination chemotherapy. Cancer Res. 2001;61:1527–32.
16. Ogawa T, et al. Osteoblastic differentiation is enhanced by rapamycin in rat osteoblast-like osteosarcoma (ROS17/2.8) cells. Biochem Biophys Res Commun. 1998;249:226–30.
17. Seufferlein T, Rozengurt E. Rapamycin inhibits constitutive p70s6k phosphorylation, cell proliferation, and colony formation in small cell lung cancer cells. Cancer Res. 1996;56:3895–7.
18. Grewe M, et al. Regulation of cell growth and cyclin D1 expression by the constitutively active FRAP-p70s6K pathway in human pancreatic cancer cells. Cancer Res. 1999;59:3581–7.
19. Pang H, Faber LE. Estrogen and rapamycin effects on cell cycle progression in T47D breast cancer cells. Breast Cancer Res Treat. 2001;70:21–6.
20. van der Poel HG, et al. Rapamycin induces Smad activity in prostate cancer cell lines. Urol Res. 2003;30:380–6.
21. Busca R, et al. Inhibition of the phosphatidylinositol 3-kinase/p70 (S6)-kinase pathway induces B16 melanoma cell differentiation. J Biol Chem. 1996;271:31824–30.
22. Muthukkumar S, et al. Rapamycin, a potent immunosuppressive drug, causes programmed cell death in B lymphoma cells. Transplantation. 1995;60:264–70.
23. ICH Q1A (R2). International conference on harmonization of technical requirements for the registration of drugs for human use. Stability testing of new drug substances and products Q1A (R2) (2003).
24. Silva-Junior AA, et al. Thermal behavior and stability of biodegradable spray-dried microparticles containing triamcinolone. Int J Pharm. 2009;368:45–55.
25. ANVISA, Brasil. Resolução RDC n° 58, December 20, 2013. Brasília, DF: D.O.U; 2013.
26. ICH Q1B. International conference on harmonization of technical requirements for the registration of drugs for human use. Stability testing: photostability testing of new drug substances and products Q1B (1996).
27. United States Pharmacopoeia. 31st ed. Rockville: United States Pharmacopeial Convention (2008).
28. ANVISA, Brasil. Resolução RE n° 1, July 29, 2005. Brasília, DF: D.O.U; 2005.
29. Kim C. Advanced pharmaceutics: physicochemical principles. New York: CRC Press; 2004.
30. Rodrigues PO, et al. Aplicação de Técnicas Termoanalíticas na Caracterização, Determinação da Pureza e Cinética de Degradação da Zidovudina (AZT). Acta Farm Bonaer. 2005;24:383–7.
31. Medeiros ACD, et al. Thermal stability of prednisone drug and tablets. J Therm Anal Calorim. 2001;64:745–50.
32. Souza NAB, et al. Thermal stability of metronidazole drug and tablets. J Therm Anal Calorim. 2003;72:535–8.
33. Souza FS, et al. Correlation studies between thermal and dissolution rate constants of cimetidine drug and tablets. J Therm Anal Calorim. 2003;72:549–54.
34. Cides LCS, et al. Thermal behaviour, compatibility study and decomposition kinetics of glimepiride under isothermal and non-isothermal conditions. J Therm Anal Calorim. 2006;84:441–5.
35. Yoshida MI, et al. Thermal analysis applied to verapamil hydrochloride characterization in pharmaceutical formulations. Molecules. 2010;15:2439–52.
36. Yoshida MI, et al. Thermal behavior study and decomposition kinetics of amiodarone hydrochloride under isothermal conditions. Drug Dev Ind Pharm. 2011;37:1–10.
37. Yoshida MI, et al. Thermal characterization of lovastatin in pharmaceutical formulations. J Therm Anal Calorim. 2011;106:657–64.
38. Oliveira MA, et al. Análise térmica aplicada à caracterização da sinvastatina em formulações farmacêuticas. Quím Nova. 2010;33:1653–7.
39. Oliveira MA, et al. Análise térmica aplicada a fármacos e formulações farmacêuticas na indústria farmacêutica. Quím Nova. 2011;34:1224–30.
40. Mattos JR, et al. Análise Térmica (TG, DSC e DTA). São Paulo: USP; 1995.
41. Zech SG, et al. Identification of novel rapamycin derivatives as low-level impurities in active pharmaceutical ingredients. J Antibiot. 2011;64:649–54.
42. Sobhani H, et al. A reversed phase high performance liquid chromatographic method for determination of rapamycin. Iran J Pharm Res. 2013;12:77–81.
43. Dantas HJ. Dissertation. Estudo termoanalítico cinético e reológico de biodiesel derivado do óleo de algodão (*Gossypium hisutum*). Universidade Federal da Paraíba (UFPB), João Pessoa, PB (2006).
44. Hughes P, et al. The isolation, synthesis and characterization of an isomeric form of rapamycin. Tetrahedron Lett. 1992;33:4739–42.
45. Ribani M, et al. Validação em métodos cromatográficos e eletroforéticos. São Paulo: Quím Nova; 2004. p. 27.
46. Galwey AK, Brown ME. Analysis and interpretation of experimental kinetic measurement. In: Thermal decomposition of ionic solids: chemical properties and reactivities, Vol. 5 1999; p. 139–171
47. Costa IM. Dissertation. Estudo de propriedades físico-químicas de metalofármacos de dirutênio com anti-inflamatórios não esteroídes. Universidade de São Paulo (USP), São Paulo, SP (2014).
48. Salvio Neto H. Dissertation. Estudo de compatibilidade fármaco/excipiente e de estabilidade do prednicarbato por meio de técnicas termoanalíticas, e encapsulação do fármaco em silica mesoporosa do tipo SBA—15. Universidade de São Paulo (USP), São Paulo, SP (2010).
49. Brown ME. Introduction to thermal analysis: techniques and applications. 2nd ed. New York: Kluwer Academic Publishers; 2001.